1. SCIENTIFIC RESEARCH

CONDENSED MATTER PHYSICS

The main objectives of research in the framework of the theme involved the application of neutron scattering techniques and complementary methods to investigate the structure, dynamics and microscopic properties of nanosystems and novel materials, which are of great importance for the development of nanotechnologies in the fields of electronics, pharmacology, medicine, chemistry, modern condensed matter physics and interdisciplinary sciences. In view of the IBR-2 reactor shutdown for modernization, the experimental activities conducted by the personnel of the FLNP Department of Neutron Investigations of Condensed Matter (NICM) were carried out in neutron and synchrotron centers in Russia and abroad. These activities were performed in accordance with the Topical Plan for JINR Research and International Cooperation under the existing cooperation agreements and accepted beam time application proposals. The activities on the IBR-2 reactor were carried out in accordance with the modernization program plan for the spectrometers. Most attention was given to the realization of the top priority projects (construction of the new DN-6 diffractometer for studying microsamples, multipurpose GRAINS reflectometer and modernization of the SKAT/EPSILON spectrometers for geophysical research).

Within the framework of investigations under the theme, the employees of the NICM Department maintained broad cooperation with many scientific organizations in Russia and abroad. The cooperation, as a rule, was documented by joint protocols or agreements. In Russia, particularly active collaboration was with the thematically close organizations, such as RRC KI, PNPI, MSU, IMP, ISSP RAS, IC RAS, and others.

A list of main scientific topics studied by the employees of the NICM Department includes:

- Investigation of structure and properties of novel crystal materials and nanosystems by neutron diffraction;
- Investigation of magnetic colloidal systems in bulk and at interfaces;
- Investigation of structure of carbon nanomaterials;
- Magnetism of layered nanostructures;
- Investigation of supermolecular structure and functional characteristics of biological, colloidal and polymeric nanodispersed materials;
- Investigation of nanostructure and properties of lipid membranes and lipid complexes;
- Investigation of atomic dynamics of nanosystems and materials by neutron inelastic scattering;
- Investigation of texture and properties of minerals and rocks;
- Analysis of internal stresses in bulky materials and factory-made goods.

Scientific results.

Structure investigations of novel oxide materials.

The magnetic and crystal structures of the complex cobalt oxide $Pr_{0.5}Sr_{0.5}CoO_3$ have been studied using neutron diffraction and synchrotron radiation in the temperature range from 1.5 to

1120 K. Unlike other $Ln_{0.5}Sr_{0.5}CoO_3$ compounds, it exhibits both a paramagnetic-ferromagnetic transition at $T_C \approx 226$ K and one more magnetic phase transition at $T_A \approx 120$ K accompanied by a change in the behavior of magnetization in external magnetic fields and an anomalous behavior of elastic properties of the material. Successive structural transitions with the reduction of the crystal symmetry from cubic (space group $Pm\bar{3}m$) to rhombohedral ($R\bar{3}c$), then to orthorhombic (Imma) and triclinic ($P\bar{1}$) are detected at temperatures of about 800, 300 and 120 K (**Fig. 1**). The obtained results have helped to refine the earlier suggested models of the crystal structure of various phases. The anomalies in the temperature behavior of some interatomic distances and angles, as well as the reorientation of cobalt magnetic moments are observed at the transition to $P\bar{1}$ phase.

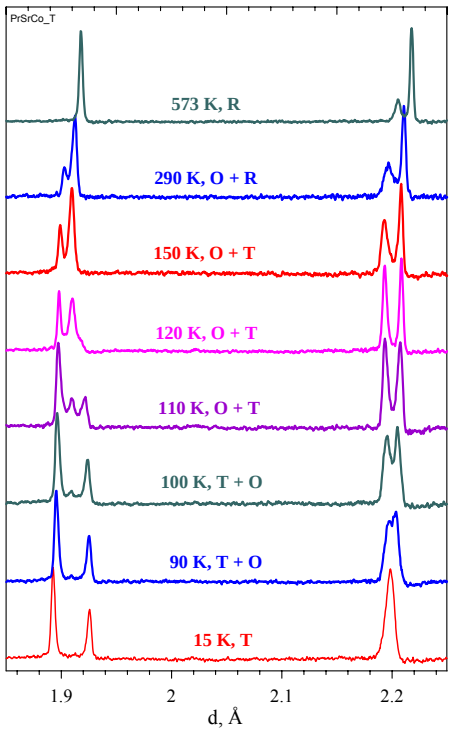

Fig. 1. A characteristic section of the diffraction spectrum of $Pr_{0.5}Sr_{0.5}CoO_3$ measured on the HRFD diffractometer at various temperatures. The temperature (from 15 K to 573 K) and corresponding structural phases: R = $R\bar{3}c$, O = *Imma*, T = $P\bar{1}$ are indicated.

The atomic and magnetic structures of $La_{0.5}Ca_{0.5}CoO_3$ cobaltite have been studied by the neutron diffraction technique at high pressures of up to 4 GPa in the temperature range from 10 to 300 K [1]. The Curie temperature increases with the pressure with the coefficient $dTC/dP = 1$ K/GPa, demonstrating the stability of the ground ferromagnetic (FM) state. The pressure dependence of the ground FM state in $La_{0.5}Ca_{0.5}CoO_3$ is in drastic contrast with that for $La_{1-x}Ca_xCoO_3$ at a lower calcium content ($x < 0.3$). For the latter compound, under pressure the suppression of the ground FM state and a large negative pressure coefficient of the Curie temperature ($dT_C/dP < 0$) are observed. The pressure dependences of the structural parameters have been obtained.

The structural and magnetic phase transitions in the multiferroic $BiMnO_3$ complex oxide have been studied at high pressures (**Fig. 2**) [2]. A unique feature of this compound as compared to other multiferroics is the combination of magnetoelectric effects with ferromagnetic ordering. A structural phase transition between two monoclinic modifications of *C2/c* symmetry was observed at a pressure of 1 GPa, which was accompanied by a significant change in the parameters of the unit cell and some interatomic distances. The structural phase transition occurs with a change in the character of

magnetic ordering from ferromagnetic (T_C = 100 K) to antiferromagnetic (T_N = 90 K) one with a

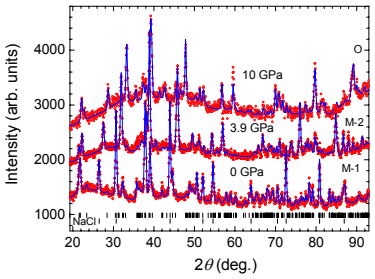

Fig. 2. Neutron diffraction spectra of $BiMnO_3$ obtained at various pressures and room temperature at the HRPT diffractometer (PSI, Switzerland) and treated by the Rietveld method (left). Magnetic structure of the high pressure monoclinic phase of $BiMnO_3$ (right).

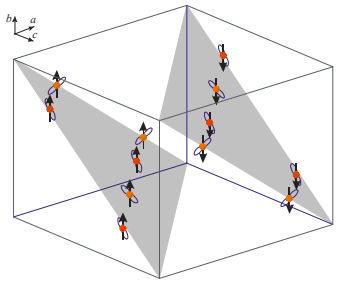

propagation vector k = (½ ½ ½). With a further increase in pressure at $P \sim 8$ GPa a structural phase transition to an orthorhombic phase of *Pbnm* symmetry was observed. The obtained results made it possible to reveal the role of competing superexchange interactions in the mechanism of occurrence of magnetoelectric phenomena.

Investigations of magnetic fluids.

Within the framework of the Helmholtz Association (Germany)-RFBR (Russia) Joint Research Groups (project HRJRG-16) structural characteristics of biocompatible ferrofluids synthesized for treating human brain cancer tumors have been determined using small-angle neutron scattering [4, 5]. The double layers of myristic (MA+MA) or lauric (LA+LA) acids were used to stabilize magnetite nanoparticles (size of ~10 nm, polydispersity > 50%) in a liquid medium. Despite rather large volume fractions of dispersed magnetite ($\varphi_m \sim 10$ %) on retention of a high stability the presence of nanoparticle clusters with a characteristic size of 30-40 nm has been revealed in the samples. The use of the contrast variation (H_2O/D_2O mixtures) and the application of the method of modified basic functions have allowed us to determine the cluster characteristics related to their inner structure. In particular, a significant difference in the surfactant fraction in the clusters has been observed for the samples of two types. It has been found that the clusters in the samples of the LA+LA type consist of magnetite particles completely coated with a surfactant shell about 3.5 nm thick, while in the samples of the MA+MA type the clusters comprise magnetite particles partially coated with the surfactants (**Fig. 3**). This indicates that more significant aggregation of the surfactant with a larger length decreases MA adsorption on the magnetite surface during the preparation. This conclusion is consistent with the fact that the synthesis of stable aqueous ferrofluids with the use of longer surfactants from the series of monocarboxylic acids (palmitic and stearic acids) is impossible. Other important characteristics obtained in the research are the temperature stability of the clusters and the absence of micelles of free (non-adsorbed) surfactants, which distinguishes the systems under study from the previously studied technical water-based ferrofluids stabilized by dodecylbenzenesulphonic acid, where fractal aggregates and significant surfactant excess with the micelle formation were observed.

The contrast variation in small-angle neutron scattering (Helmholtz Centre Geesthacht) using the method of modified basic functions has been applied in research of biocompatible ferrofluids prepared by the replacement of sodium oleate with polyethyleneglycol when stabilizing magnetite in water (Institute of Experimental Physics, Kosice, Slovakia) [6].

The cluster reorganization has been revealed depending on the amount of the polymer added to the system. In particular, under sufficient polymer concentration in the initial ferrofluid compact clusters (size 40 nm) transform to extended fractal clusters (size above 120 nm).

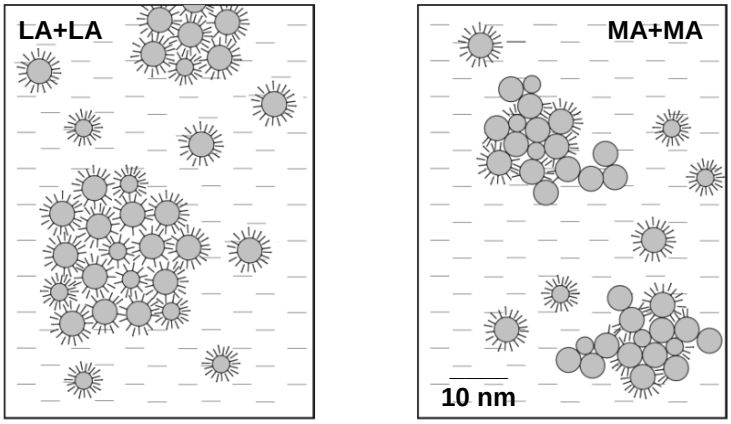

Fig. 3. A schematic representation of the cluster structure in two biocompatible aqueous ferrofluids with double layer stabilization of magnetite nanoparticles by lauric (LA+LA) and myristic (MA+MA) acids on the basis of contrast-variation small-angle neutron scattering data. Illustration by Yu.I.Emelina (FLNP JINR).

Along with this, the thickness of the stabilizing shell changes slightly, which is indicative of the polymer adsorption in the flat configuration on the magnetite surface. Taking into account a decrease in the saturation magnetization of the new fluid it is concluded the observed reorganization is related to the lowering of the system stability.

Investigations of carbon nanomaterials.

In the frame of the research of fullerene solutions with moderate polarity (dielectric constant 10–50) the C_{60}/N-methyl-pyrrolidone (C_{60}/NMP) system has been thoroughly investigated. The solution is characterized by the formation of large (size up to 500 nm) but stable clusters of fullerene molecules within about one month after the dissolution. In particular, it has been proposed [7] to follow the cluster growth by means of the extraction into an organic solvent immiscible with NMP (e.g. hexane) (**Fig. 4**). The cluster formation is correlated with the temporal solvatochromic effect (change in UV-Vis absorption spectrum with time). It has been shown that after the dissolution C_{60} is extracted from C_{60}/NMP (mauve color) to hexane (mauve color of lower intensity) in the molecular state. The extraction decreases with time and finally shows that all C_{60} in C_{60}/NMP (brownish yellow color) transfer to the unextractable clusters. The transition from a molecular to a colloidal (cluster) solution is reflected in mass-spectra of dried solutions. On addition of water (immiscible with hexane either) to the system the extraction resumes, which suggests that the clusters are destroyed as a result of the detachment of single C_{60} molecules. The appearance of separate molecules in the solution has been testified by mass-spectrometry, and a decrease in the cluster size has been detected by small-angle neutron scattering. It has been shown that along with this, water molecules chemically bind fullerene (charge-transfer complex). So, basing on the complex analysis and combining various methods, the solvatochromic effects in the C_{60}/NMP and C_{60}/NMP/water systems have been explained: together with the cluster development the initial fullerene-solvent complexes change with time (preferably on the cluster surface), thus favoring the fullerene dissolution in the NMP/water mixture.

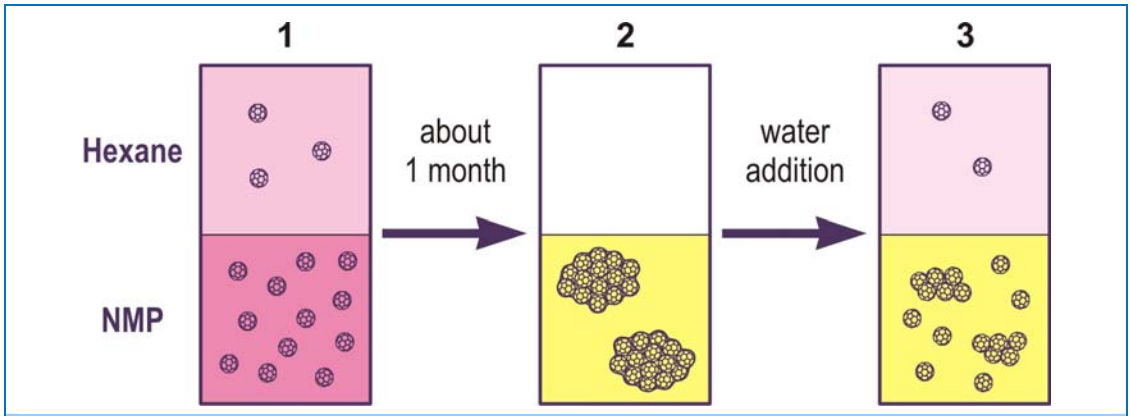

Fig. 4. A schematic representation of various stages in the extraction of fullerene C_{60} from C_{60}/NMП and C_{60}/NMП/H_2O solutions using the data of complementary structural methods. Cluster sizes are in the ranges of 100-500 nm (stage 2) and 10-100 nm (stage 3). Illustration by Yu.I.Emelina (FLNP JINR).

The theoretical model of the cluster formation in polar solutions of fullerene C_{60} has been developed [8]. The experimental data for C_{60}/NMP solution have been analyzed in terms of the kinetic theory of nucleation. It has been shown that in the frame of the nucleation theory, similar to the case of non-polar C_{60} solutions, the application of the cluster drop model results in fast phase separation in the system. The use of estimated thermodynamic parameters for the solution C_{60}/NMP in the kinetic equations gives ~10 μs for the duration of the independent growth stage. In contrast to non-polar solutions, the limited growth model, which limits the cluster size (the aggregation number), is inapplicable from the physical viewpoint. For the qualitative description of the processes in the system an alternative mechanism of the limited growth has been proposed. It assumes that the gradual formation of donor-acceptor complexes C_{60}-NMP restricts the growth of fullerene clusters. The corresponding model takes into account the assumed change of the C_{60}-NMP complexes with time.

Investigations of magnetic layered nanostructures.

The experimental investigations of the predicted inverse proximity effect for a superconductor-

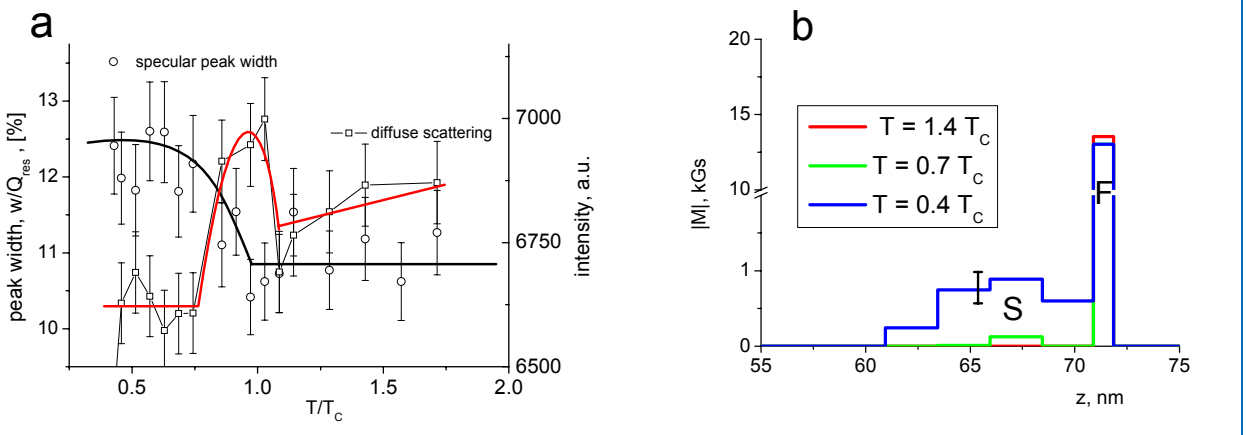

Fig. 5. a) Temperature behavior of magnetic scattering intensities near the superconducting phase transition.
b) Magnetic profile of the system above and below the transition temperature.

ferromagnet bilayer of the V/Fe nanostructure, which consists in the appearance of magnetization in the superconductor (**Fig. 5**) have been carried out. Theoretical predictions gave both the positive (in respect of ferromagnetic magnetization direction) and negative magnetization of the superconductor. The studies of the V/Fe bilayer have revealed the inverse proximity effect [9]. It has been found that below the superconducting transition temperature the superconducting layer is magnetized positively and the ferromagnetic layer — negatively, so the whole bilayer increases its magnetic moment.

Investigations of lipid membranes and lipid complexes.

Aqueous solutions of multilamellar vesicles (MLV) of the membranes modeling the lipid component in the mucous membranes of the oral cavity of mammals based on ceramide-6 and membranes in its structure (mixtures of sphingomyelin/dipalmitoylphosphatidylcholine/ dipalmitoylphosphatidylethanolamine with ceramide-6), have been investigated by means of synchrotron radiation diffraction in the temperature range of 20 - 80 (90)^{o}C (**Fig. 6**).

It has been found that at high temperatures (70-80 ^{o}C) the mixture of sphingomyelin /phospholipids tends to form an inverse hexagonal phase. Ceramide-6 at a mole fraction of 0.2-0.3 increases the repeat distance in MLV of the sphingomyelin/phospholipids mixture by ~1 Å and hinders the formation of the inverse hexagonal phase at high temperatures.

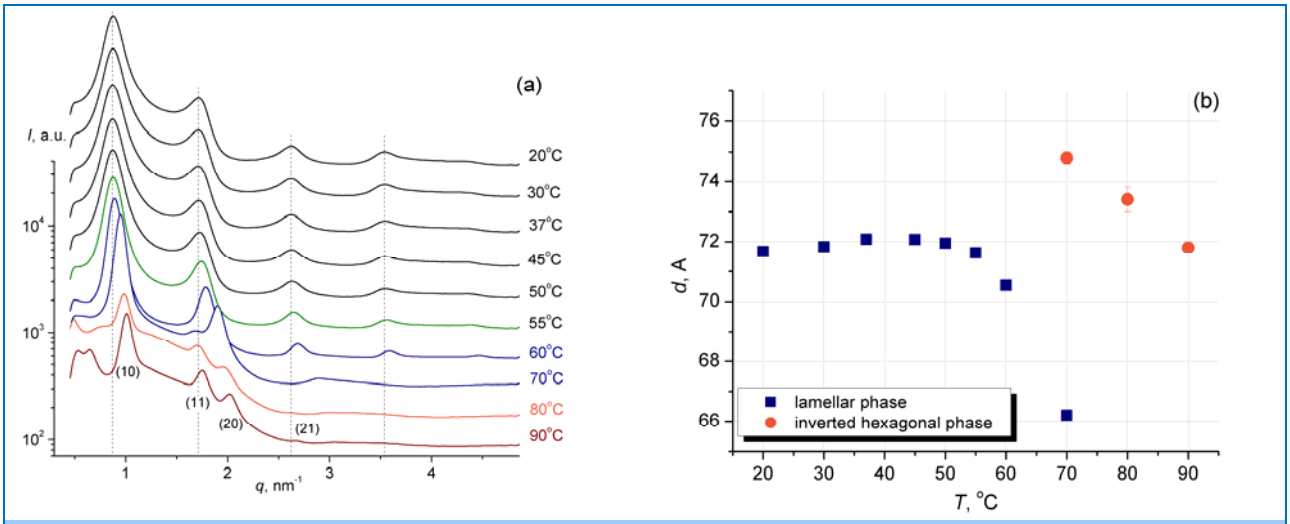

Fig. 6. (a) Diffraction spectra of the lamellar structure of MLV of sphingomyelin/DPPC/DPPE = 1/2/2. (b) Temperature dependence of the repeat distance (d) of the lamellar phase (■) and the parameter ($a = 2d/\sqrt{3}$) of the inverted hexagonal phase (●) of MLV of sphingomyelin/DPPC/DPPE = 1/2/2

As a result of the performed studies of the membranes composed of ceramide 6/cholesterol/ palmitic acid/cholesterol sulfate it has been found that the phase state of the membrane depends not only on the temperature, but also on the pH of water used in their preparation. At low pH values (5-7), the lipid bilayer is in the L_{φ} crystal phase and with increasing pH up to 9 there occurs a phase transition to the L_{β} gel phase while the degree of order of hydrocarbon tails decreases significantly and the membrane becomes single-phase.

The preparation phosphogliv dissolved in water has been studied. It has been determined that the lipid fraction of phosphogliv exists in an aqueous phase in the form of multilamellar liposomes with a repeat distance of 47.1 Å, which consist of the mixture of phosphatidylcholine (PC) and glycyrrhizic

acid (GRA). In the precipitate liposomes with repeat distances of 47.1 Å (mixture of PC and GRA) and 62.8 Å (pure PC) have been found.

The phospholipid transport system developed in the Institute of Biomedical Chemistry of the Russian Academy of Medical Sciences has been investigated. Samples were prepared by dissolving a lyophilized preparation in water with a drug concentration of 25 %. This concentration corresponds to the medical recommendation on the use of the medicine. The studies have demonstrated that 25 % solution of PTNS in water is a vesicle system of low polydispersity and the relative standard deviation in size is 20-30 %. The average radius of the vesicle is 160 Å, which corresponds to the PTNS nanoparticle size of 320 Å. The morphology of PTNS has been determined. It has been proved that the phospholipid transport system is a vesicle system with a low level of polydispersity at its 25 % concentration in water.

Investigations of polymer and colloidal nanosystems.

In cooperation with the Enikolopov Institute of Synthetic Polymer Materials of RAS and Bogoliubov Laboratory of Theoretical Physics (BLTP) of JINR the investigation of structural features of dendrimers — polymers combining properties of hyperbranched macromolecules and particles — has been continued [10]. For small-angle neutron scattering using the contrast variation technique the average scattering density of dendrimers has been determined and the invariants have been calculated. It has been shown that the scattering density distribution in the dendrimer volume is uniform within the experimental error. The upper estimate of the inhomogeneity of the scattering density of the dendrimers has been obtained. The possibility of the penetration of the solvent into the dendrimers has been demonstrated and the quantitative estimate of the volume accessible for the penetration of the solvent has been given. Some generalizing conclusions about the structure and properties of the specified kind of dendrimers from lower to higher generations have been made. In the dendrimer-solvent system at various concentrations and external conditions the existence of a structural factor, which is not typical for the «rigid sphere» systems has been revealed down to the lowest concentrations.

Theoretical calculations on the simulation of small-angle scattering from deterministic fractals — generalized Cantor fractals — have been performed in cooperation with BLTP JINR (**Fig. 7**) [11]. Deterministic fractals are a model of strictly self-similar structures of nano-objects, which nowadays can be obtained due to the development of modern nanotechnologies. The fractal dimension can vary from zero to three depending on the degree of its packing, which is controlled by the dimensionless scaling factor. The form-factor of the generalized Cantor fractal has been calculated analytically for arbitrary values of the wave vector and any finite iterations of the fractal, which makes it possible to use it for describing small-angle neutron and X-ray scattering from orientationally-ordered sets of fractals. For randomly oriented mono- and polydisperse fractals the scattering intensity has been obtained in the form of simple integrals. The values of the asymptotes for the fractal structure factor have been calculated and the radius of gyration has been obtained analytically for arbitrary iteration. The “shelf” behavior of the small-angle scattering curve has been explained. The possibility to estimate the number of particles from which the fractal is formed has been demonstrated.

In the framework of the study of surfactant solutions used for stabilizing ferrofluids, the structure and interaction parameters of micelles of dodecylbenzenesulfonic acid (DBSA) in deuterated water have been studied by small-angle neutron scattering (Helmholtz Center Geesthacht) [12]. The dependences of the micellar aggregation number, fractional charge, charge per micelle and surface potential on the surfactant concentration are analyzed. A typical increase in the micelle size with the

growth in the acid content has been found, which can be related to the transition from spherical to rod-like micelles.

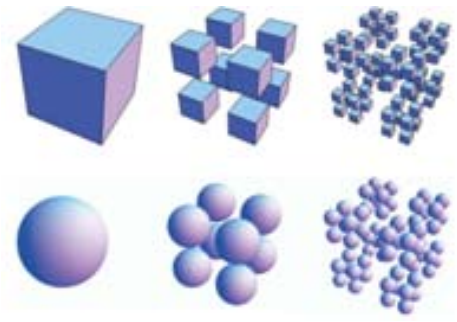

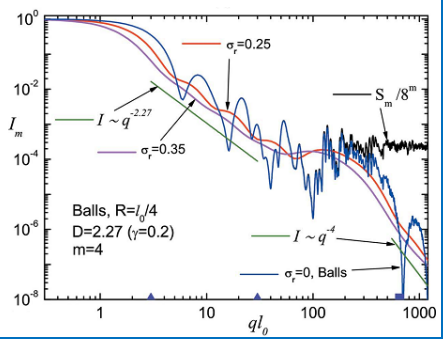

Fig. 7. Model representation of zero, first and second iterations for the generalized Cantor set composed of cubes and balls (left) and model intensity curves with the fractal dimension D = 2.27 with regard to polydispersity (right).

The obtained data have been used for estimating concentrations of micelle and free surfactant in bulk of aqueous ferrofluids (magnetite in water with a double shell of DBSA under excess).

Atomic dynamics.

The spin dynamics in the $Ce_{(1-x)}Y_xAl_3$ system at a transition from a heavy fermion (HF) state at x=0 to a mixed valence (MV) state at x=0.5 has been investigated by inelastic neutron scattering [13] (**Fig. 8**). It has been shown that the substitution of yttrium for cerium results in a strong transformation of spectrum components of the magnetic response due to an increase in the *k-f* hybridization.

The dynamics of uranium mononitride, which is considered to be a basic material for the creation of combined fuel for fast neutron reactors has been investigated. The inelastic neutron scattering spectra of UN have revealed quasi-resonant peculiarities in the region of the gap between acoustic and optical vibrations, which can be explained by solitons and nonlinear localized modes.

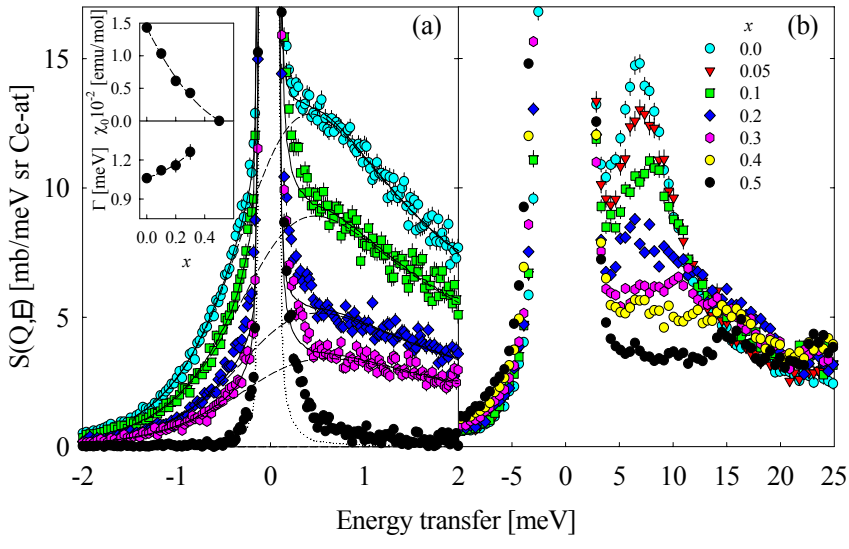

Fig. 8. S(Q,ω) of $Ce_{1-x}Y_xAl_3$ as a function of yttrium concentration "x":

a) measured on IN6 (ILL, France) at an average scattering angle of 60° and an incident energy of 3.12 MeV. The solid lines are fits to a quasielastic Lorentzian lineshape (dashed line) and an elastic peak (dotted line) convolved with the resolution function. The inset shows the dependence of yttrium concentration "x" on the values of the static susceptibility, ω_0, (top inset) and the half-width, $\Gamma/2$, (bottom inset) of the quasielastic peaks.

b) measured on LRMECS (ANL, USA) at an average scattering angle of 15° and an incident energy of 35 MeV.

Atomic structure and lattice dynamics of nickel hydroxide, $Ni(OH)_2$, an electrode material for chemical current sources, have been investigated by incoherent inelastic neutron scattering. The

comparative analysis of the vibrational spectra and lattice dynamics of nickel and magnesium hydroxides has been performed on the basis of inelastic incoherent neutron scattering data as well as Raman and IR-spectroscopy [14]. Optical phonon spectra have been calculated using the methods of the density functional theory and agree well with the vibrational spectroscopy data. The analysis of the calculated force constant matrix has made it possible to suggest the interpretation of the main features in the spectra of these compounds. The density functional method provides an insight into the peculiarities of interatomic interactions characteristic for these layered compounds and shows the important role of the spin-spin interactions in nickel hydroxide. It has been demonstrated that this method can be successfully applied to the investigation of the atomic structure and lattice dynamics of the β-NiOOH phase.

Applied research.

Among traditional applied investigations in the Department of Neutron Investigations of Condensed Matter are the experimental studies of internal stresses and texture of rocks and minerals, determination of internal stresses in bulk materials and products, including engineering materials and components of machines and devices. For the most part, these investigations are carried out using neutron diffraction.

Experiments to study elastic wave propagation in model inhomogeneous anisotropic media —

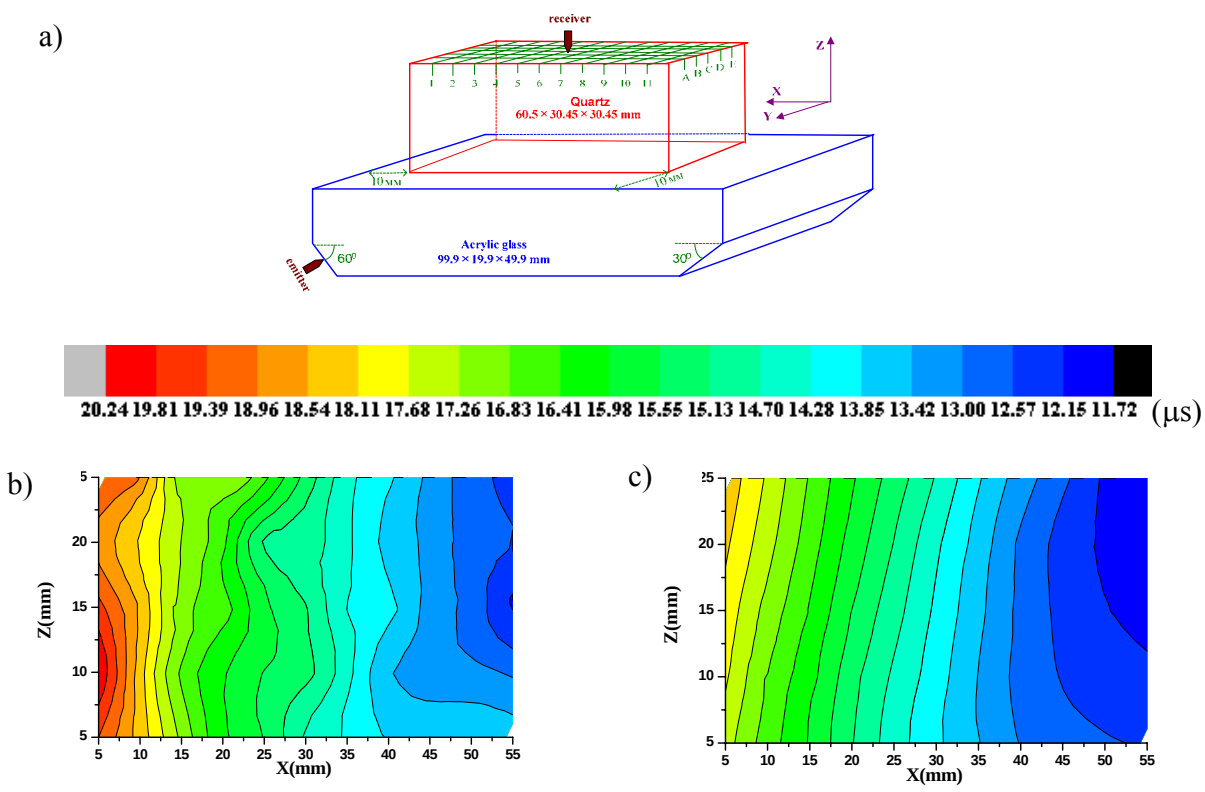

Fig. 9. (a) Scheme of a two-layer model of acrylic glass and quartz with the indicated location of ultrasound emitters and receiver. Isoline distribution maps of travel times of quasi-compressional waves in the model of acrylic glass and quartz. The quartz single crystal is in contact with the glass surface by the **XZ** plane; the emitter is attached to the side cut of the glass plate made at an angle of 60° to the horizontal surface: b) ultrasound frequency is 200 kHz; c) ultrasound frequency is 5 MHz.

samples of acrylic glass + single-crystal quartz, acrylic glass + polycrystalline graphite (with the known texture), epoxy resin + biotite — have been carried out (**Fig. 9**). It has been shown that in the model materials of "epoxy resin + biotite" differing by an order of magnitude in the grain size of biotite (0-0.4 mm and 2-5 mm), the velocities of longitudinal elastic waves with various frequencies coincide. It has been suggested that the discrete wavelet-transform method be used for the analysis of acoustic signals and determination of transverse elastic wave velocities. The comparison of theoretical calculations with the ultrasonic data from physical models has been conducted and a satisfactory agreement of the results has been obtained.

Neutron diffraction studies of residual stresses in a cross-shaped sample of austenitic stainless steel AISI 321 (**Fig. 10**) subjected to biaxial stress-strain cycling have been carried out. Under the action of plastic deformation the austenite matrix underwent partial transformation, which caused the formation of a new ferromagnetic martensitic phase in the sample. The total residual stresses in both phases of the cycled sample were measured using the time-of-flight neutron diffraction technique. Their analysis in the planar approximation has made it possible to determine macrostresses (similar in both phases) and microstresses (in each phase separately) as well as the contribution of hydrostatic pressure to the total phase stresses. In addition, it has been found that during planar cycling there occurs a partial transition from the martensitic phase to the austenitic one, which is connected with a plastic deformation of the material.

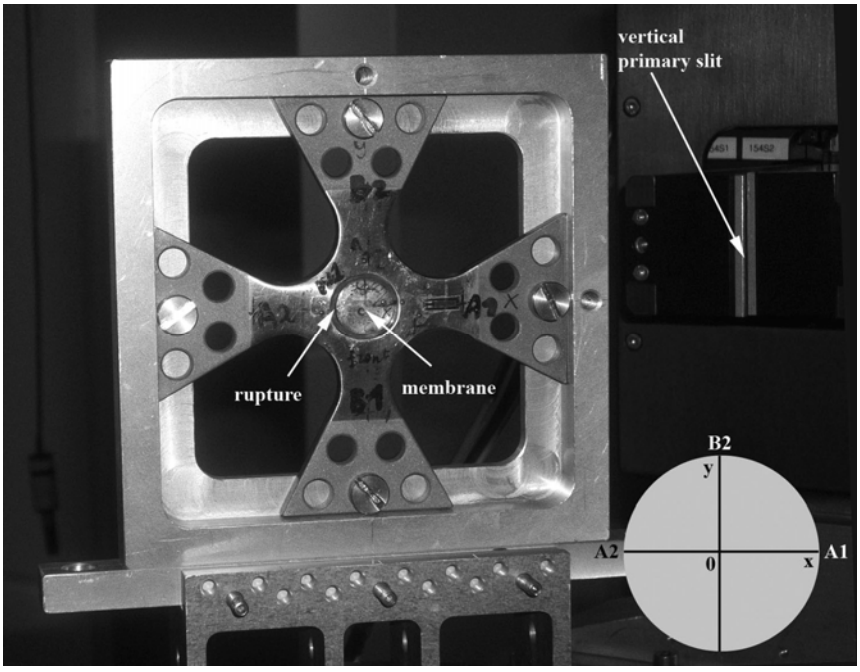

Fig. 10. A photo of the cross-shaped sample of austenitic stainless steel AISI 321 prepared for measuring internal stresses at the POLDI spectrometer (PSI, Switzerland). A vertical beam-forming slit is indicated by the arrow.

The studies of crystallographic texture and residual stresses in reactor materials, specifically in cylindrical fuel plugs made of E-110 alloy for the VVER-1000 reactor have continued. It has been demonstrated that the manufacturing process of parts by rotational swaging results in the formation of an axial crystallographic texture, which undergoes significant changes at annealing. Residual stresses of the first kind in cold-worked (strain of ≈ 150 MPa in a radial direction) and annealed (residual stresses are close to zero) fuel plugs have been calculated.

Using the data analysis of the texture measurement of polyphase granite gravel from the Erzgebirge, the magmatic flow and oriented crystal growth in an anisotropic stress field have been demonstrated to be the major texture formation processes. Texture measurements of rock salt from different sources in North Germany have been performed to study active deformation mechanisms. Despite the presence of external deformation, preferred grain orientations have not been determined. It has been concluded that during deformation processes texture does not develop or previously existing texture is destroyed because of the grain boundary migration processes.

The modeling of elastic wave velocities in rocks on the basis of the texture data of rock samples has shown that the elastic properties of rocks are independent of the influence of crack formation at high pressures. The experimental estimates of elastic wave velocities at low pressures have been compared with the crack formation effects, the extrapolation on high pressures is necessary to evaluate pressure conditions at very great depths. The further investigations have confirmed that all the model functions used are inapplicable for extrapolation. A refinement procedure for a model function, which will result in a better extrapolation of velocities has been suggested.

A texture study of marble samples using the neutron diffraction technique has been performed on TEX-2 (FRM-I) of the GKSS Research Center and STRESS SPEC (FRM-II) of the Technical University of Munich, Germany. The marble samples are from the Carrara region (Italy). This is a topical problem, since it is necessary to establish the reason for deformation and decay of the plates made of this kind of marble. These plates are widely used in Germany for cladding buildings (for example, the University Library building in Göttingen). The decay is caused by the accumulation of

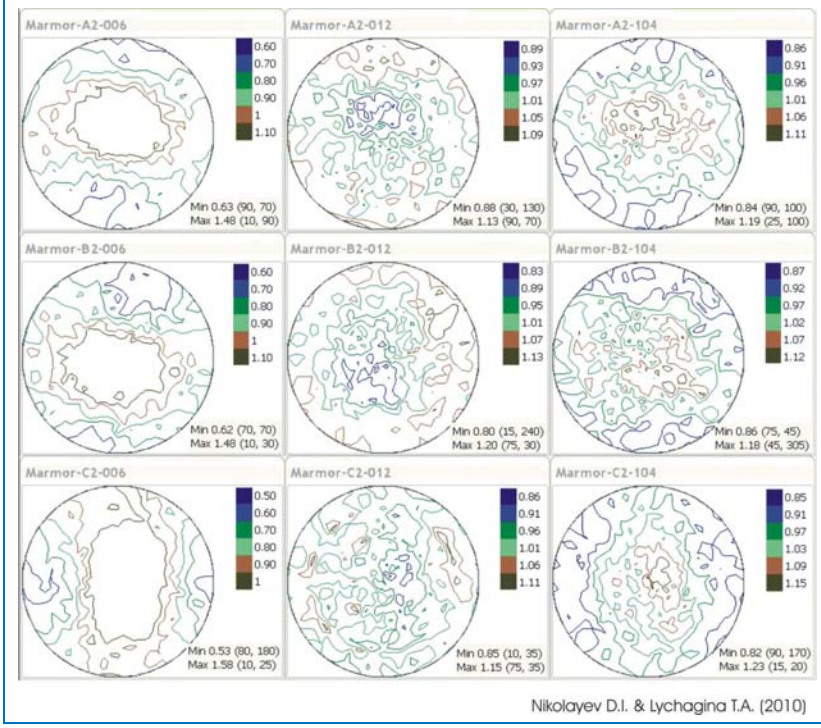

Fig. 11. Pole figures of the marble sample from the Carrara region (Italy) obtained using the diffraction data measured on the TEX-2 diffractometer (FRM-II, Germany).

residual stresses under cyclic deformation (as a result of the action of seasonal temperature gradients).

On the basis of the performed investigations (**Fig. 11**) it has been concluded that the texture sharpness

in the marble samples under study is insufficient to have a significant effect on the formation of the residual stress distribution. Nevertheless, the deformation and decay of marble plates is observed and it is necessary to find the reason for these phenomena; for this purpose it is planned to carry out a number of experiments and simulation studies.

Instrument development.

The installation of the beam chopper and the head part (**Fig. 12**) of the mirror neutron guide for the new DN-6 diffractometer for microsample investigations has been completed on beam 6b of the IBR-2 reactor. The manufacturing of mirrors for the tail part of the neutron guide has continued. The technical documentation for manufacturing the mechanical part of DN-6 has been prepared. The manufacturing of a gas position-sensitive detector has started in the FLNP Spectrometers' Complex Department (SCD).

Fig. 12. The head part of the mirror neutron guide installed on beam 6 of the IBR-2 reactor in the framework of the realization of the project of construction of the new DN-6 diffractometer for microsample investigations.

The installation of the head part (**Fig. 13**) of the new multifunctional reflectometer GRAINS on beam 10 of the IBR-2 reactor has been completed. The vacuum housing (**Fig. 13**) of the beam-forming system has been manufactured, assembled and tested for vacuum. The manufacturing of the background neutron drum chopper with a horizontal slit and the construction of an autonomous vacuum

Fig. 13. The head part of the GRAINS reflectometer installed in the ring corridor of the IBR-2 reactor (left) and the ready-assembled vacuum housing of the beam-forming system (during tests for vacuum in SPA «Atom», right).

system for the reflectometer have continued. The designing and manufacturing of a control system for stepper motors of the instrument and the software for the reflectometer has started. A 2D position-sensitive neutron detector has been manufactured and tested (in cooperation with SCD).

The effect of gravity on the resolution function of a reflectometer with a horizontal sample plane has been studied. The dependences of gravitational distortions of the specular reflection coefficient on various parameters of the reflectometer (collimation, sample sizes, relative distances between the elements of the reflectometer) have been obtained and analyzed.

The activities to install and vacuumize the splitter (**Fig. 14**) on beam 7 of IBR-2, which splits an initial neutron beam into three independent beams for the EPSILON, SKAT and NERA spectrometers, have been completed. A new background chopper with a wide window for three neutron guides has been installed, assembled and tested (in cooperation with SCD). Three lambda-choppers for the 7A-1 (EPSILON), 7A-2 (SKAT) and 7B (NERA) neutron guides have been manufactured and delivered. The technical documentation and the contract to manufacture 80-m sections of a mirror vacuum neutron guide for the NERA spectrometer have been prepared. The activities to modernize the spectrometers on beam 7 are carried out in cooperation with SCD.

Fig. 14. The splitter dividing the initial neutron beam into three independent beams for the EPSILON, SKAT and NERA spectrometers (left) and the new background chopper (right) on beam 7 of the IBR-2 reactor.

Work on the installation and adjustment of mechanical units and mirror segments of a neutron concentrator for the DIN-2PI spectrometer has been completed.

A project of the creation of a neutron spectrometer for studying transient processes in real time at the IBR-2 reactor has been prepared.

Theoretical and experimental activities to substantiate a new method of studying nanostructures — neutron magnetic resonance — have been conducted. The method is based on the phenomenon of neutron wave splitting in the processes of reflection and refraction of neutrons in a static collinear magnetic field and oscillating magnetic field perpendicular to it, which is connected with a gain (loss) of a quantum of an electromagnetic wave to (from) a neutron. This phenomenon in the neutron reflection channel was discovered in the measurements on the REMUR spectrometer in 2006 and verified in 2010 in the investigations in Germany (Munich). At the same time it has been shown that the reflection has a resonance character (intensity of off-specularly reflected neutrons depends on the frequency of the oscillating field and grows at a frequency equal to the Larmor frequency of the neutron spin precession around the magnetic field induction vector in a film).

The development work on the production of polarized neutron microbeams to study local inhomogeneities of nanostructures has been performed (**Fig. 15**). In conventional neutron experiments the information obtained on the object under study is averaged over the width of the incident beam (size of 0.1-1 mm). Layered waveguides, which are a three-layer film structure that transforms a rather wide (0.1 mm) and collimated (0.01°) beam into a narrow (0.1 μm) and divergent (0.1°) one, hold much promise for producing narrower neutron beams (neutron probe). Using layered waveguides the polarized neutron microbeams 0.15 μm wide have been produced for the first time. The neutron beam has the form of an elongated slit, therefore it may be most effectively used for one-dimensional lattices in the form of strips of magnetic materials.

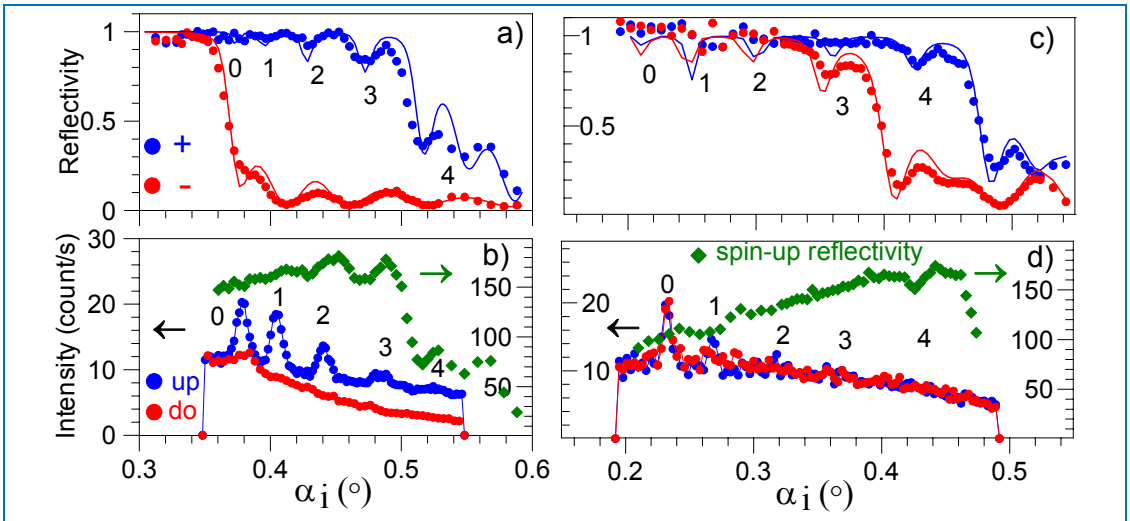

Fig. 15. Production of polarized neutron microbeams using magnetic layered structures. Left column: polarizing waveguide FeO_x(5.4 nm)/Fe(15 nm)/Cu(136 nm)/Fe(51 nm)//glass. Right column: non-polarizing waveguide Py(13 nm)/Al(141 nm)/Py(48 nm)//glass. Top: Reflection coefficients of spin states «+» and «–». The dots are the experimental data; the lines are the fits of the model structure. Indices denote minima that correspond to the resonances of the neutron wave function in the waveguide layer of Cu or Al. Bottom: maxima of the neutron microbeam as a function of the grazing angle of the initial neutron beam. For comparison purposes the intensity of the specularly reflected beam is given. The position of maxima of the microbeam corresponds to the position of minima of the specularly reflected beam. The width of the microbeam is equal to the width of the waveguide layer of Cu(136 nm) and Al(141 nm).

The experimental study of the influence of the finite thickness of spin-flippers with rotating magnetic fields on their efficiency has been carried out at the FRMII reactor, Germany. Similar devices can be used in spin-echo spectrometers of a new type. The finite thickness of the flippers makes it impossible to produce an exact neutron spin flip by 180°.

The automatic high-hydrostatic-pressure device at the YuMO spectrometer for carrying out volumetric studies in the pressure range of 0-4 kbar and in the temperature range of 5-200 °C has been modernized. First P-V-T experiments with water solutions of dimyristoylphosphatidylcholine have been conducted.

References

1. N.O.Golosova, D.P.Kozlenko, E.V.Lukin, B.N.Savenko. "Effect of high pressure on the crystal and magnetic structures of $La_{0.5}Ca_{0.5}CoO_3$ cobaltite", JETP Letters, v. 92, pp. 114-118 (2010).

2. D.P.Kozlenko, A.A.Belik, S.E.Kichanov, I.Mirebeau, D.V.Sheptyakov, Th.Straessle, O.L.Makarova, A.V.Belushkin, B.N.Savenko, E.Takayama-Muromachi. "Competition between ferromagnetic and antiferromagnetic ground states in $BiMnO_3$ at high pressures", Phys. Rev. B 82, 014401 (6 pp.) (2010).

3. A.V.Belushkin and D.P.Kozlenko Structural organization of nanomaterials and nanosystems: neutron scattering insight, Advances in Natural Sciences: Nanoscience and Nanotechnology 1, 023002 (8 pp.) (2010).

4. M.V.Avdeev, B.Mucha, K.Lamszus, L.Vekas, V.M.Garamus, A.V.Feoktystov, O.Marinica, R.Turcu, R.Willumeit. "Structure and in vitro biological testing of water-based ferrofluids stabilized by monocarboxylic acids". Langmuir, 26 (2010) pp. 8503-8509.

5. M.V.Avdeev, V.L.Aksenov. "Small-angle neutron scattering in structure research of magnetic fluids. Review", UFN, v. 180, №10, pp. 1009-1034 (2010).

6. M.V.Avdeev, A.V.Feoktystov, P.Kopcansky, G.Lancz, V.M.Garamus, R.Willumeit, M.Timko, M.Koneracka, V.Zavisova, N.Tomasovicova, A.Jurikova, K.Csach, L.A.Bulavin. "Structure of water-based ferrofluids with sodium oleate and polyethylene glycol stabilization by small-angle neutron scattering: contrast-variation experiments". J. Appl. Cryst. 43 (2010) 959–969.

7. O.A.Kyzyma, M.V.Korobov, M.V.Avdeev, V.M.Garamus, S.V.Snegir, V.I.Petrenko, V.L.Aksenov, L.A.Bulavin. "Aggregate development in C_{60}/N-metyl-2-pyrrolidone solution and its mixture with water as revealed by extraction and mass spectroscopy", Chem. Phys. Lett. 493, 103–106 (2010).

8. M.V.Avdeev, T.V.Tropin, V.L.Aksenov. "Models of cluster formation in solutions of fullerenes", Russian Journal of Phys. Chem. 84(8), 1273–1283 (2010).

9. V.L.Aksenov, Yu.N.Khaidukov, Yu.V.Nikitenko. "Peculiarities of magnetic states in "Ferromagnet-Superconductor" heterostructures due to proximity effects", Journal of Physics: Conference Series, 211, 012022-012027 (2010).

10. A.V.Rogachev, A.I.Kuklin, A.Yu.Cherny, A.N.Ozerin, A.M.Muzafarov, E.A.Tatarinova, V.I.Gordeliy. "Structure of organosilicon dendrimers of higher generations", Physics of the Solid State, 52, № 5, 1045-1049 (2010).

11. A.Yu.Cherny, E.M.Anitas, A.I.Kuklin, M.Balasoiu and V.A.Osipov. "Scattering from generalized Cantor fractals". J. Appl. Cryst. 43, 790–797 (2010).

12. V.I.Petrenko, M.V.Avdeev, V.M.Garamus, L.A.Bulavin, V.L.Aksenov, L.Rosta. "Micelle formation in aqueous solutions of dodecylbenzene sulfonic acid studied by small-angle neutron scattering", *Coll. Surf. A* 369 (2010) 160–164.

13. E.A.Goremychkin, R.Osborn, I.L.Sashin, P.Riseborough, B.D.Rainford, D.T.Adroja, J.M.Lawrence. "Transition from heavy-fermion to mixed-valence behavior in Ce_{1-x} Y_xAl_3: a quantitative comparison with the Anderson impurity". Phys. Rev. Lett. 104, 176402 (4 pp.) (2010).

14. V.Yu.Kazimirov, M.B.Smirnov, L.Bourgeois, L.Guerlou-Demourgues, L.Servant, A.M.Balagurov, I.Natkaniec, N.R.Khasanova, E.V.Antipov. "Lattice dynamics of Ni and Mg hydroxides". Solid State Ionics, 181, 1764-1770 (2010).